The magnetic behaviors of the metamagnetic and ferromagnetic phases of $[Fe(C_5Me_5)_2][TCNQ]$ (TCNQ = 7,7,8,8-tetracyano-*p*-quinodimethane). Determination of the phase diagram for the metamagnetic phase†

Michelle L. Taliaferro,[a] Fernando Palacio[b] and Joel S. Miller*[a]

Received 28th February 2006, Accepted 16th March 2006
First published as an Advance Article on the web 18th April 2006
DOI: 10.1039/b603016e

The detailed magnetic behaviors of the ferro- (**1FO**) and metamagnetic (**1MM**) phases of $[FeCp^*_2][TCNE]$ (Cp^* = pentamethylcyclopentadienide; TCNE = tetracyanoethylene) aligned parallel to the applied magnetic field, H, were obtained using eicosane (**E**). The T_c for **1FO** is 3.1 K from the maximum in the frequency independent $\chi'(T)$ data and 3.0 K from the maximum in the $C_p(T)$ data, and exhibits a hysteresis with a coercive field, H_{cr}, ~ 50 Oe, a remanent magnetization of 1900 emu Oe mol^{-1} at 2 K, and saturation magnetization of 16 740 emu Oe mol^{-1}. Significant differences were observed between aligned **1MM** (**1MM + E**) and unaligned samples. Metamagnetic **1MM + E** saturates to 15 900 emu Oe mol^{-1}, and has a 1300 Oe critical field at 2 K that decreases with increasing temperature. The 2 K $M(H)$ of **1MM + E** displays a small bump between |3000 and 4000| Oe that is not observed in **1MM**. The T_c for **1MM + E** is 2.5 ± 1 K from the maximum in the frequency independent $\chi'(T)$ data, and peak maximum in $C_p(T)$ data. The lack of a $\chi''(T)$ response for $H = 0$ is in accord with **1MM + E** having an antiferromagnetic ground state. Upon application of an applied field a $\chi''(T)$ signal appears and increases in intensity until 1500 Oe in accord with **1MM + E** going from an antiferromagnetic to a ferromagnetic-like state. For $H >$ 1500 Oe the $\chi''(T)$ signal decreases. In contrast to **1MM**, between 2.2 and 2.8 K $\chi'(H)$ and $\chi''(H)$ exhibit peaks between 3000 and 4000 Oe. The temperature at which the peak maximum in $C_p(T)$ occurs (2.4 K) for **1MM** and is unexpectedly independent of H. The peak maxima observed in $\chi'(T,H)$ at 100 and 1000 Hz were use to construct a magnetic phase diagram, $H(T)$, for metamagnet **1MM + E**, which has three different magnetic phases: paramagnetic, antiferromagnetic, and an intermediate phase. The detailed magnetic characterization of the structurally similar **1MM** and **1FO** phases will provide a basis for theorists to understand the subtle spin exchange interactions that lead not only to magnetic ordering, but the type of the ordering.

Introduction

Organic-based materials exhibiting cooperative physical properties form an important contemporary research thrust in chemistry, materials science, and physics.[1] Today examples of organic-based superconductors[2] and magnets,[3] *e.g.*, materials where p-electrons from organic specie(s) play an active role in the physical properties, are well documented. The first organic-based magnet, $[Fe^{III}Cp^*_2]^{\bullet+}[TCNE]^{\bullet-}$ (Cp^* = pentamethylcyclopentadienide; TCNE = tetracyanoethylene), was reported in 1985[4,5] and magnetically orders as a ferromagnet below a T_c of 4.8 K.[6,7] Earlier, $[Fe^{III}Cp^*_2]^{\bullet+}[TCNQ]^{\bullet-}$ (TCNQ = 7,7,8,8-tetracyano-*p*-quinodimethane) was reported to order as a metamagnet below 2.55 K.[8,9] In addition to the TCNE and TCNQ electron transfer salts of $Fe^{II}Cp^*_2$ the magnetic properties of numerous other salts have been reported.[10]

$[FeCp^*_2][TCNQ]$, **1**, is now known to form three different magnetic phases: a paramagnet,[9] a ferromagnet, **1FO**, with T_c = 3.1 K,[11] and the aforementioned metamagnet,[9] **1MM**. Both **1FO** and **1MM** form as $\cdots D^+A^-D^+A^-\cdots$ chains in which $[FeCp^*_2]^{\bullet+}$ ($D^{\bullet+}$) and $[TCNQ]^{\bullet-}$ ($A^{\bullet-}$) alternate. Only a few key structural differences exist. For **1FO** the cation C_5Me_5 rings are in an eclipsed conformation whereas in **1MM** they are staggered. More significantly, some differences are also present in the interstack arrangements of **1FO** and **1MM**. Most notable the $[TCNQ]^{\bullet-}$ anions of **1FO** zigzag in the *b* direction whereas in **1MM** they do not zigzag, but are arranged in the same direction.[11] Also, the closest N···N $[TCNQ]^{\bullet-}\cdots[TCNQ]^{\bullet-}$ distance in **1FO** is 4.337 Å and is 4.080 Å for **1MM**. Since this distance is closer in **1MM** than in **1FO**, **1MM** is likely to have stronger antiferromagnetic coupling.[6,12] The field dependent magnetization, $M(H)$, of **1MM** reveals that below 1500 Oe **1MM** is in an antiferromagnetic state, switching to a ferromagnetic-like state above this field.[11] The temperature dependence of $M(H)$ of **1MM** shows that as the temperature increases the critical field, H_c, decreases along with the sharpness of the transition. Hence, based on the $M(H,T)$ responses, it is described as a metamagnet.

[a]*Department of Chemistry, University of Utah, 315 S. 1400 E. RM 2020, Salt Lake City, UT 84112-0850, USA*
[b]*Instituto de Ciencia de Materials de Aragon, CSIC-Univ. de Zaragoza, P. Cerbuna 12, Zaragoza 50009, Spain*
† This article is part of a themed issue on Molecular Magnetic Materials.

The magnetic phase diagrams of antiferromagnets have been classified into two classes each having a characteristic $H(T)$ behavior when their axis of antiparallel alignment is oriented parallel to the applied field.[13] Class 1 antiferromagnets are highly anisotropic with a field-induced first order phase transition ($T < T_N$) arising from the reversal of the local spin directions. For historical reasons this sudden reversal of the local spins is called a *metamagnetic* phase transition and Class 1 antiferromagnets are described as *metamagnets*. A typical $H(T)$ phase diagram for a Class 1 antiferromagnet contains both antiferromagnetic and paramagnetic regions (Fig. 1a), as observed for $FeCl_2$, $DyPO_4$, and $[\{(323)Ni\}_3\{Fe^{III}(CN)_6\}_2]_n \cdot 12H_2O$[14] (323 = *N*,*N*′-bis(3-aminopropyl)ethylenediamine). Note that the first order boundary line of the metamagnetic transitions does not limit the whole antiferromagnetic region in the magnetic phase diagram (broken line in Fig. 1a). Indeed, it extends from $T = 0$ K up to the so called tricritical point, $T_T < T_N$; above T_T and up to T_N the transition from the antiferromagnetic state to the paramagnetic one is second order (solid line in Fig. 1a).

In contrast, Class 2 antiferromagnets are isotropic or weakly anisotropic and their characteristic magnetic phase diagram defines three regions, namely, antiferromagnetic, paramagnetic, and spin flop regions. Upon application of a magnetic field a Class 2 antiferromagnet undergoes a first order phase transition, due to the flopping of the spins to orient perpendicular to the applied field. This transition, which is customarily known as a *spin-flop* transition, defines the boundary between the antiferromagnetic and the spin flop regions (broken line in Fig. 1b). In the spin flop region the effect of the applied magnetic field results in the rotation of spins from an antiparallel to a parallel state. Typical examples of Class 2 antiferromagnets are MnF_2,[15a] and the $A_2FeCl_5 \cdot H_2O$ (A = K, Rb)[15] family of antiferromagnets (Fig. 1b). Due to significant anisotropy of $[Fe^{III}Cp^*_2]^{\bullet+}$ [16] Class 1 metamagnetic behavior is anticipated.

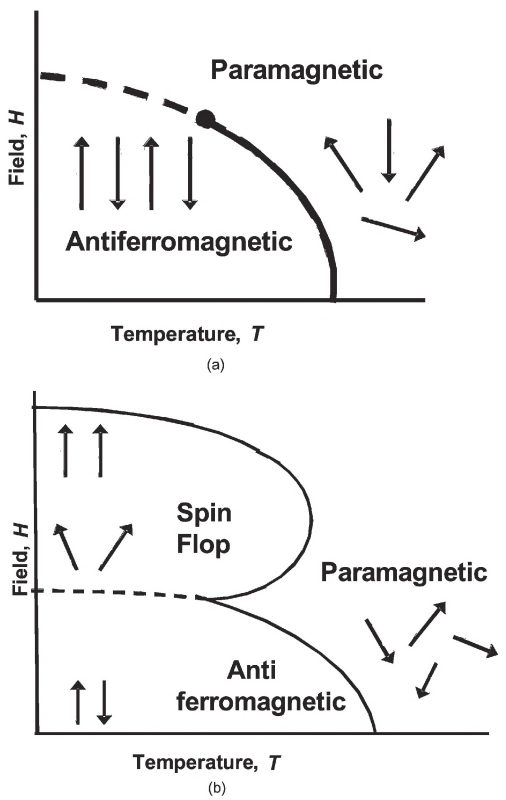

Fig. 1 $H(T)$ phase diagram for Class 1 (a) and Class 2 (b) metamagnets. Adapted from ref. 13. First and second order transitions are denoted by (- - - -) and (—), respectively.

Herein, we report the detailed magnetic properties and temperature dependences of the specific heat for both **1FO** and **1MM**, and the $M(H)$ phase diagram for **1MM** is constructed and discussed in context of previously reported phase diagrams for antiferromagnets, where **1MM** is best described as an antiferromagnet with a metamagnetic-like transition.

It should also be noted that the profound differences in the magnetic properties for **1FO** and **1MM** must be a consequence of subtle differences in their respective structures that lead to differing magnitudes of antiferromagnetic and ferromagnetic couplings. Hence, the detailed magnetic characterization of the **1FO** and **1MM** polymorphs, along with their structures,[9,11] provide a basis for theorists to understand the subtle spin coupling interactions that lead not only magnetic ordering, but also the sign of the ordering.

Experimental

Synthesis

$FeCp^*_2$ (Acros) was sublimed prior to use, and TCNQ was purified *via* passing through a silica column to remove any impurities present prior to use. The synthesis of $[FeCp^*_2][TCNQ]$ was carried out in an inert atmosphere (DriLab). $FeCp^*_2$ and TCNQ were reacted as previously reported[11] to form a bulk ferromagnetic phase. The bulk ferromagnetic phase was dissolved in MeCN at room temperature and allowed to stand for 2 days, and then was filtered to yield a dark green–purple powder. Magnetic measurements proved this dark green–purple powder corresponded to the **1MM** phase. To obtain the **1FO** phase the bulk ferromagnetic phase was dissolved in MeCN and warmed just before boiling. Once completely dissolved the solution was placed in the freezer (−20 °C) and allow to stand for 6 weeks. The purple crystals that precipitated were collected *via* vacuum filtration.[17] Magnetic measurements proved these purple reflecting crystals corresponded to the **1FO** phase.

Physical methods

All AC and DC magnetic measurements were taken on a 90 kOe Quantum Design (QD) Physical Property Measurement System (PPMS) as previously reported.[18] AC magnetic measurements were done between 2 and 5 K and between 0 and 5000 Oe with a 5 Oe drive field. DC magnetic measurements were done between 2.0 and 2.6 K and between ±50 kOe. All magnetic measurements were taken in gelatin capsules.

All heat capacity measurements were made on a PPMS as a function of field ($\leqslant$5000 Oe) between 2 and 20 K. Both **1FO** and **1MM** were studied as pressed pellets that were attached *via* Apiezon M grease to the sample platform. The sample thermometer was calibrated at each field used prior to running

the experiment to avoid magnetoresistance effects. An Apiezon M grease addenda file was measured at each field prior to the sample being adhered to the sample platform and studied. The addenda files were used to correct for the raw heat capacity data from the heat capacity of the grease and the sample platform.

Infrared spectra (400 to 4000 $\pm$ 1 cm^{-1}) were obtained on a Bruker Tensor 37 spectrophotometer as potassium bromide pellets. Both **1FO** and **1MM** exhibit ν_{CN} at 2177 and 2153 cm^{-1} indicative of the $[TCNQ]^{\bullet -}$ radical anion; thus, IR cannot be used to distinguish between **1FO** and **1MM**.

Sample preparation

As sufficiently large single crystals of **1MM** were not available, a polycrystalline sample of **1MM** ($\sim$15 mg) was mixed with eicosane ($\sim$30 mg) in a mortar and pestle (T_m = 310 K),[19] and placed inside a gelatin capsule and loaded into the PPMS. The mixture was heated to 317 K in zero applied field, after which a field of 90 kOe was applied to align the crystals parallel to the field, and the sample was further heated to 320 K. The magnetization as a function of decreasing temperature was then monitored by observing the raw magnetization (M) data between 320 and 280 K. Initially M decreased upon cooling until the sample reached 310 K, then M stabilized and began to increase as 280 K was approached. The sample was then cooled slowly in a 90 kOe field at a rate of 2 K min^{-1} and upon reaching 100 K the 90 kOe field was oscillated back to zero to avoid a remanent magnetic field. The sample was further cooled at 10 K min^{-1}, until 2 K was reached, and then the magnetic studies were initiated.

Results and discussion

The reaction of $FeCp^*_2$ and TCNQ forms three polymorphs of $[FeCp^*_2][TCNQ]$ composition. Paramagnetic $\{[FeCp^*_2]^+\}_2[TCNQ]_2^{2-}$ is the thermodynamically stable polymorph.[8] Nonetheless, the 1-D chain structured $[FeCp^*_2]^+[TCNQ]^-$ meta- (**1MM**) and ferromagnetic (**1FO**) polymorphs can be isolated, and were independently studied.

Ferromagnetic phase, 1FO

In order to compare the magnetic data of **1FO** to the results reported for the single crystal of $[FeCp^*_2][TCNE]$,[7] **1FO** was aligned parallel to the magnetic field. Due to the high anisotropy of $[FeCp^*_2]^+$ [$g_\perp \sim 1.25$ and $g_\parallel \sim 4.4$][16] **1FO** [and **1MM** (*vide infra*)] can be aligned parallel with a magnetic field using the heating/cooling protocol in eicosane (**E**), as described in the Experimental section. The value of χT at room temperature was 1.62 emu K mol^{-1} within the predicted range of 0.750 to 2.19 emu K mol^{-1} expected for **1FO**, which corresponds to g_{ave} for $[FeCp^*_2]^+$ of 3.64. From a plot of $\chi^{-1}(T)$ the Weiss constant, θ, was determined to be 24 K (T > 50 K) indicative of significant ferromagnetic coupling. However, θ is larger than the 3.8 K determined from field cooled magnetization data.[11] This difference is attributed to the alignment of **1FO**; the previous sample studied was unaligned. The field dependent magnetization, $M(H)$, at 2 K of **1FO** was characteristic of a ferromagnet and with a rapid saturation to 16,740 emu Oe mol^{-1} (Fig. 2). Unaligned **1FO** was previously reported to saturate to 11 600 emu Oe mol^{-1}.[11] From the expression for $M_s = N_A\mu_B[g_{Fe}S_{Fe} + g_{TCNQ}S_{TCNQ}]$, where N_A is Avogadro's constant, μ_B is the Bohr magneton, g_{Fe} the g-value for $[FeCp^*_2]^+$, S_{Fe} the spin for $[FeCp^*_2]^+$ (*i.e.* 1/2), g_A the g-value for $[TCNQ]^-$ (g_{TCNQ}, *i.e.* 2); and S_{TCNQ} the spin for $[TCNQ]^-$ (*i.e.* 1/2). Thus, using the M_s determined by $M(H)$ the average g_{Fe} was determined to be 3.91 for our aligned **1FO** and 2.15 for that previously reported.[7] This is similar to, but a bit lower than, 16 300 emu Oe mol^{-1} reported for a large aligned crystal of $[FeCp^*_2][TCNE]$.[7] Thus, **1FO** was almost completely aligned parallel to the magnetic field. **1FO** also displays a remanent magnetization of 1900 emu Oe mol^{-1}, and a hysteresis with a coercive field, $H_{cr} \sim 50$ Oe at 2 K (Fig. 2a). This coercivity is substantially reduced with respect to the 1000 Oe reported for $[Fe^{III}Cp^*_2]^+[TCNE]^{\bullet -}$.[7] The zero field cooled–field cooled data show a 3.0 K bifurcation temperature, and the 5 Oe $M(T)$ extrapolates to zero at 3.3 K (Fig. 3).

The $\chi_{ac}(T)$ for **1FO** exhibits both in-phase, real, $\chi'(T)$ and out-of-phase, imaginary, $\chi''(T)$ components characteristic of a noncompensated magnetic ordering in **1FO** (Fig. 4). No frequency dependence is evident and T_c taken at the temperature at which the maximum is observed in the 100 Hz data is 3.1 K. This is in close agreement with the 3.0 K T_c reported from the 175 Hz data.[11]

The temperature dependence of the heat capacity, $C_p(T)$, for **1FO** has a maximum at T_c = 3.0 K (Fig. 5). This independent determination of T_c is in excellent agreement with the value determined by $\chi_{ac}(T)$. Since no diamagnetic material isostructural to **1** is known, the lattice contribution to the specific heat could not be obtained for **1FO**, and consequently the Debye lattice specific heat could not be determined and subtracted from **1**. Thus, all heat capacity data reported are uncorrected for the lattice contribution.

Metamagnetic phase, 1MM

The room temperature value of χT for **1MM** is 1.18 emu K mol^{-1}, and following the same analysis described above for **1FO** this corresponds to g_{ave} for $[FeCp^*_2]^+$ of 2.93. Above 30 K, θ of 11.0 K is in accord with ferromagnetic coupling. For the detailed magnetic studies, **1MM** was also aligned parallel to the applied magnetic field using eicosane, *i.e.* **1MM + E**.

1MM and **1MM + E**, in contrast to **1FO**, order as antiferromagnets in zero applied field (H = 0); however, with increasing field the behavior switches to a ferromagnetic-like state, as observed in its field dependent magnetization, $M(H)$, at 2 K (Fig. 2). This behavior is characteristic of a metamagnet.[13] Unlike for **1FO**, hysteresis is not observed in **1MM** (Fig. 2c)[20a] as expected in a first order transition, the reported cases are scarce and in general no hysteresis at all is observed in antiferromagnets.[20b] The saturation magnetization (M_s) is 15 900 emu Oe mol^{-1} for **1MM + E**; hence g_{ave} is 3.70 for **1MM + E** indicative of alignment of **1MM** parallel to H in eicosane. The $M(H)$ data of **1MM + E** also contains a notable bump in the first and third quadrants between 3000 and 4000 Oe that is not observed for **1MM**. The 2.1–2.5 K $M(H)$ of

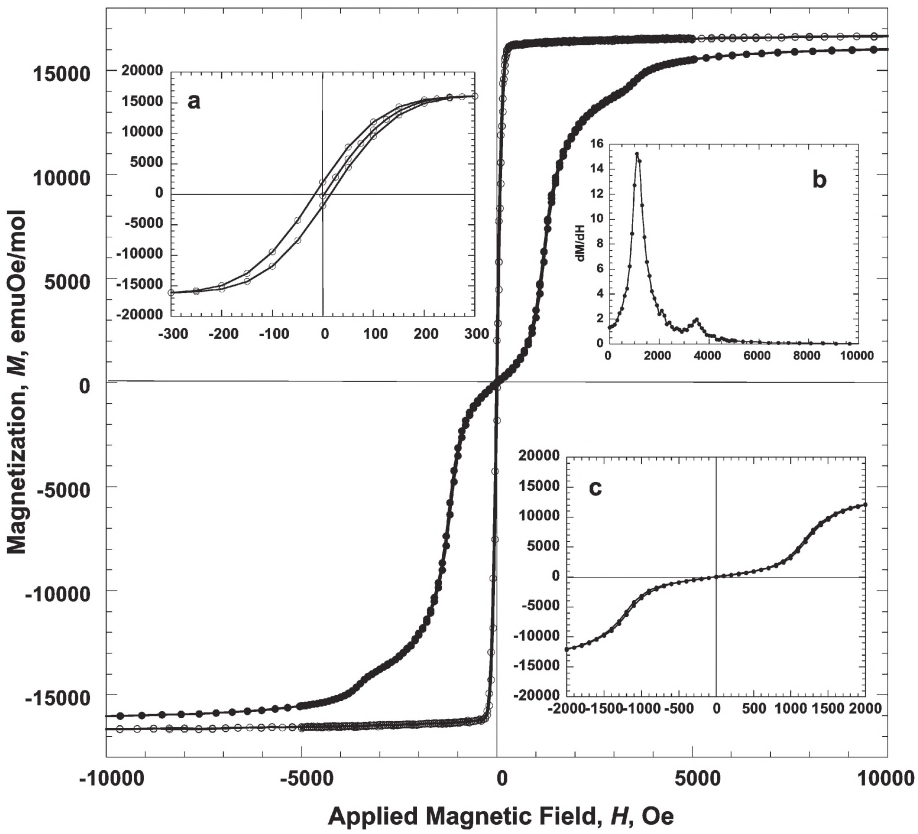

Fig. 2 2 K $M(H)$ hysteresis loops for **1FO** (○) and **1MM + E** (●). Inset are the hysteresis curve for **1FO** (a), the dM/dH of **1MM + E** (b) and the $M(H)$ curve for **1MM + E** that does not exhibit hysteresis (c).

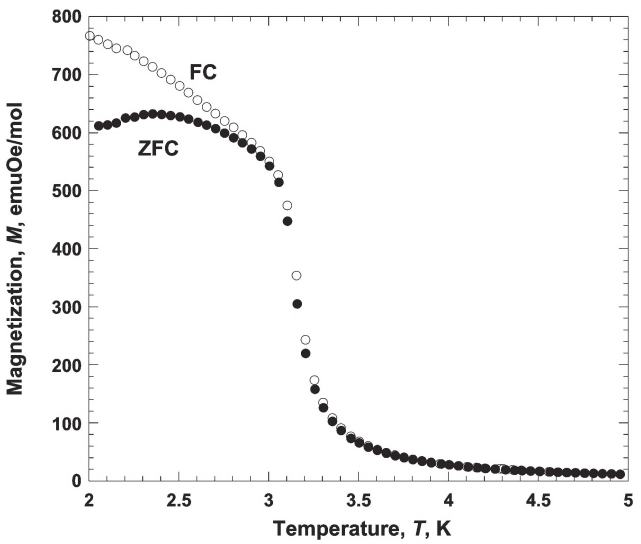

Fig. 3 5 Oe zero field (●) and field cooled (○) $M(T)$ for **1FO**.

1MM + E also displays this bump with the sharpness decreasing with increasing temperature (Fig. 6). Using the difference between the M_s values at 2 K for **1MM + E** and at the bump, ~85% of the spins can be estimated to have flipped from being antiparallel to parallel with the applied field, while the remaining −15% flipped after the bump.

The d$M(H)$/d$H(H)$ data (Fig. 2b) reveal that for the 2 K isotherm the critical field, H_c for **1MM + E** is 1300 Oe, which is in good agreement with past results.[8] The observed transition for **1MM** is sharper than that observed for **1MM + E** (Fig. 6a,b). However, both show H_c decreases nonlinearly with increasing temperature as is noted for EuSe,[21a] $CsCoCl_3 \cdot 2H_2O$,[21b] and $DyPO_4$,[21b] but differ from the linear dependence reported for [Mn^{III}porphyrin][TCNE].[22]

The frequency, f, dependence of $\chi'(T)$ and $\chi''(T)$ at zero field were determined below 5 K, and are identical for both **1MM** and **1MM + E** (Fig. 7). T_c, taken as the AC freezing temperature, T_f, at 100 Hz, was 2.6 K for **1MM + E**, and is in good agreement with the previously reported T_c of 2.55 K,[8] and no frequency dependence is present. However, the intensities differed as the response for **1MM + E** was ~5 times greater than **1MM**, as expected due to the greater alignment of the sample parallel to the applied magnetic field. The $\chi''(T)$ values for both **1MM** and **1MM + E** were essentially zero (Fig. 7) confirming that in zero field **1MM** is an antiferromagnet.

The possibility that eicosane might exert pressure on **1MM** at low temperatures and increase the T_c, as observed for THF with [$FeCp^*_2$][TCNE],[23] was ruled out after observing that repeating the same cooling procedure with [$FeCp^*_2$][TCNE], **2** (T_c = 4.8 K), no change in T_c occurred. Therefore, eicosane does not exert a pressure on **2** and by assumption on **1MM + E**.

$\chi'(T)$ and $\chi''(T)$ studies at constant field ($H <$ kOe) between 2 and 8 K and at 100, 1000 and 10 000 Hz were done on **1MM + E**. The relevance of this field range is based upon the

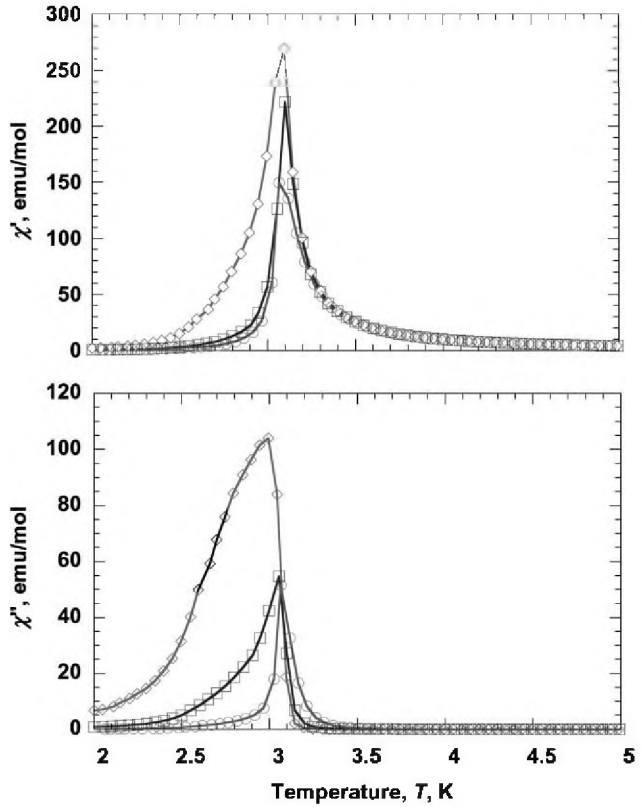

Fig. 4 $\chi'(T)$ and $\chi''(T)$ of **1FO** at 100 Hz (◇), 1000 Hz (□), and 10 000 Hz (○) (H = 0 Oe, 5 Oe drive field).

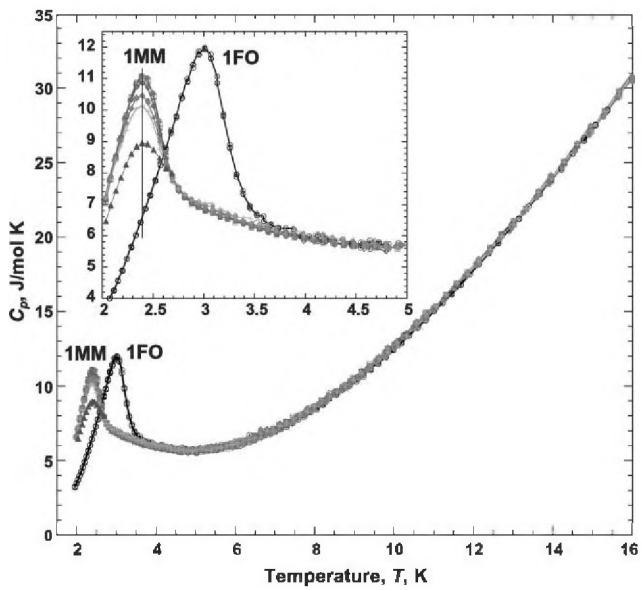

Fig. 5 Specific heat, $C_p(T)$ of **1FO** at H = 0 (○), and **1MM** at 0 Oe (●), 500 (□), 1000 (■), 1500 (◆), 2000 (◇) and 5000 Oe (▲).

2 K dM/dH *vs.* H plot (Fig. 2b). Studies showed that below 1500 Oe as the field was increased the temperature at which the maximum in $\chi'(T)$ occurred shifted to lower temperature while the intensity of $\chi''(T)$ increased. Above 1500 Oe, the temperature at which the maximum in $\chi'(T)$ occurred shifts to

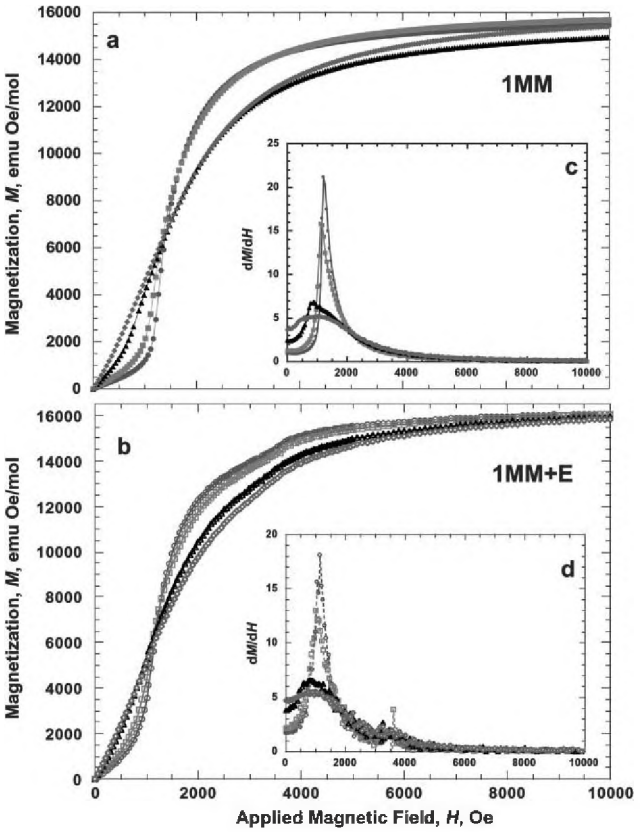

Fig. 6 $M(H)$ between 2.1 and 2.5 K of **1MM + E**: 2.1 (○) 2.2 (□) 2.4 (△) 2.5 K (◇), and **1MM**: 2.1 (●) 2.2 (■) 2.4 (▲) 2.5 K (◆). Insets are dM/dH *vs.* H for **1MM** (c) and **1MM + E** (d).

higher temperatures with increasing field, but the intensity of $\chi''(T)$ decreased.

The frequency (f) dependence of the $\chi'(T)$ was parametrized by, $\phi = \Delta T_f/[T_f \Delta \log f]$.[24] A significant frequency dependence ($\phi > 0.02$) was only observed between 1200 and 1700 Oe, and ϕ was essentially frequency independent above and below these regions (Fig. 8). For **1MM + E** $\phi < 0.005$ for $H < 1200$ Oe and $H > 1700$ Oe, between 1200 and 1700 Oe ϕ increases with increasing field to a maximum value of 0.04, consistent with **1MM + E** having a weak spin glass behavior, as disordered spin systems display $0.1 < \phi < 0.01$ as found in the alloys of PdMn (ϕ = 0.013) and NiMn (ϕ = 0.018) while the superparamagnet α-$(Ho_2O_3)(B_2O_3)$ has ϕ = 0.28.[24] The disorder in **1MM + E** can be related to spin inhomogeneities arising at the onset of the first order metamagnetic phase transition, where the spins of **1MM + E** rotate from an antiferromagnetic state to a ferromagnetic-like state as H increases. Similar behavior is also observed for **1MM**.

$\chi'(H)$ and $\chi''(H)$ studies at constant temperature ($2.0 \leqslant T \leqslant 3.5$ K) for $H \leqslant 5000$ Oe and at 100, 1000, and 10 000 Hz were carried out on **1MM + E**. The most dramatic changes were observed between 2.2 and 2.8 K, with very little frequency dependence. Thus, representative 100 Hz data reveal two peaks for $\chi'(H)$ (Fig. 9). The lower field peak, **I**, occurs between 500 and 1500 Oe, while the higher field peak, **II**, occurs between 3000 and 4000 Oe. Both shift to lower field with increasing temperature. Peak **II**, however, is not observed in **1MM**, but

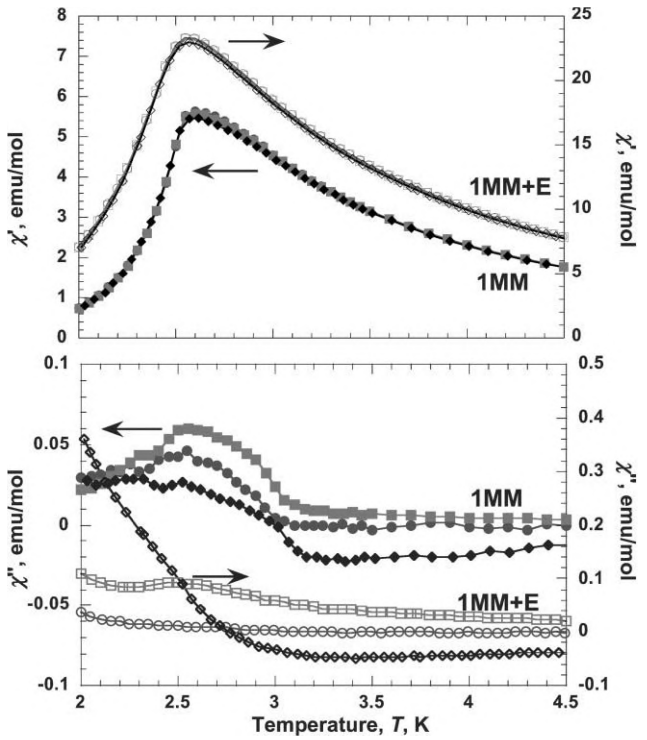

Fig. 7 $\chi'(T)$ and $\chi''(T)$ of **1MM**: (●) 100 Hz, (■) 1000 Hz, (◆) and 10000 Hz, and **1MM + E**: (○) 100 Hz, (□) 1000 Hz and (◇) 10000 Hz (H = 0 Oe, 5 Oe drive field).

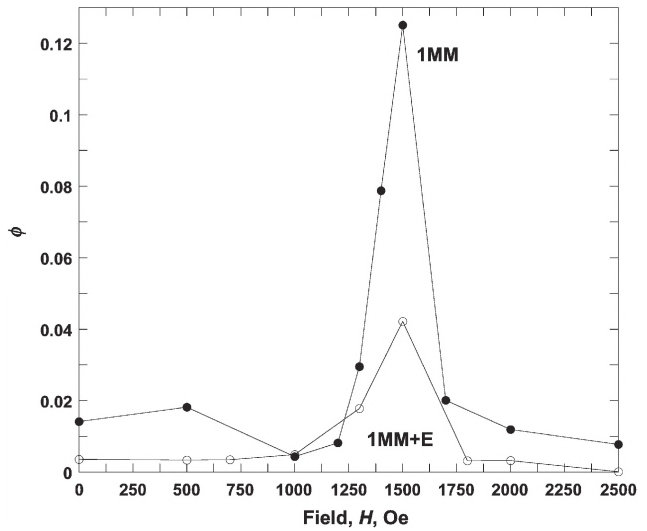

Fig. 8 $\phi(H)$ for **1MM** (●) and **1MM + E** (○). The lines are guides for the eye.

only for **1MM + E**. For the 100 Hz $\chi''(H)$ data three peaks are observed between 2.2 and 2.4 K (Fig. 10). Peak **I** occurs between 2.2 and 2.4 K in $\chi'(T)$ and corresponding to two peaks in $\chi''(H)$, with the lower field peak, **Ia**, decreasing in field as the temperature increases, and the higher field peak, **Ib**, increasing in field with increasing temperature. As the temperature increases the intensity of **Ia** decreases and becomes unobservable. Peak **II** is also present in $\chi''(H)$ between 2.2 and 2.8 K, as is seen in $\chi'(T)$.

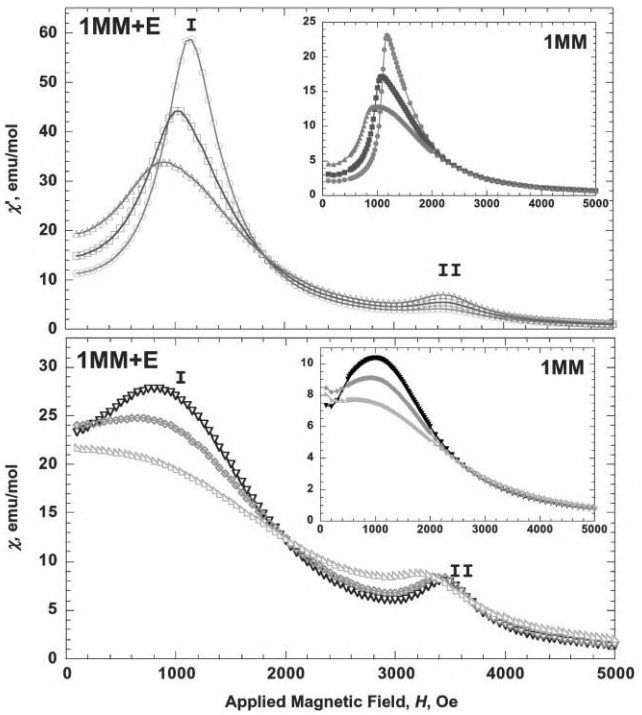

Fig. 9 2.2 to 2.8 K $\chi'(H$, 100 Hz) of **1MM + E**: (○) 2.2, (□) 2.3, (△) 2.4, (▽) 2.5, (◇) 2.6, (▷) 2.8 K, and **1MM**: (●) 2.2 K, (■) 2.3, (▲) 2.4, (▼) 2.5, (◆) 2.6, (▶) 2.8 K (H = 0 Oe, 5 Oe drive field).

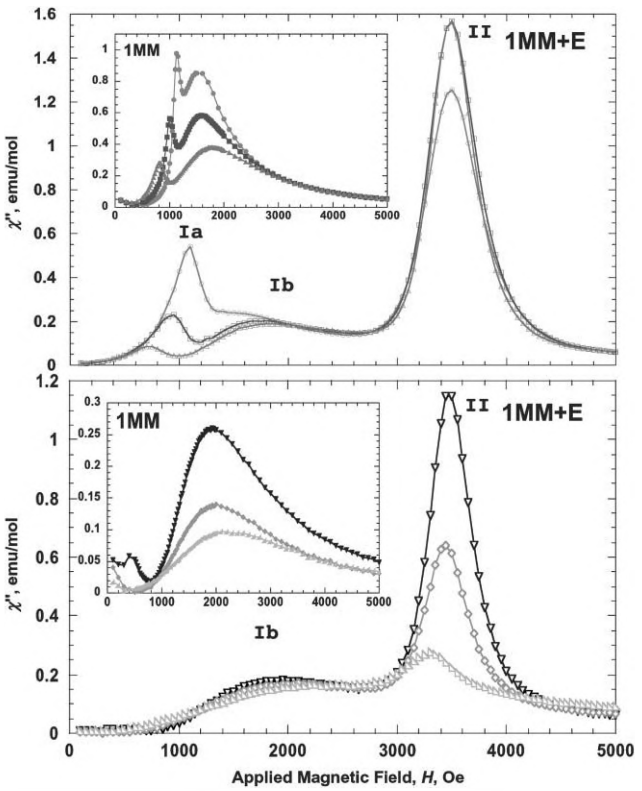

Fig. 10 2.2 to 2.8 K $\chi''(H$, 100 Hz) of **1MM + E**: (○) 2.2, (□) 2.3, (△) 2.4, (▽) 2.5, (◇) 2.6, (▷) 2.8 K, and **1MM**: (●) 2.2 K, (■) 2.3, (▲) 2.4, (▼) 2.5, (◆) 2.6, (▶) 2.8 K (H = 0 Oe, 5 Oe drive field).

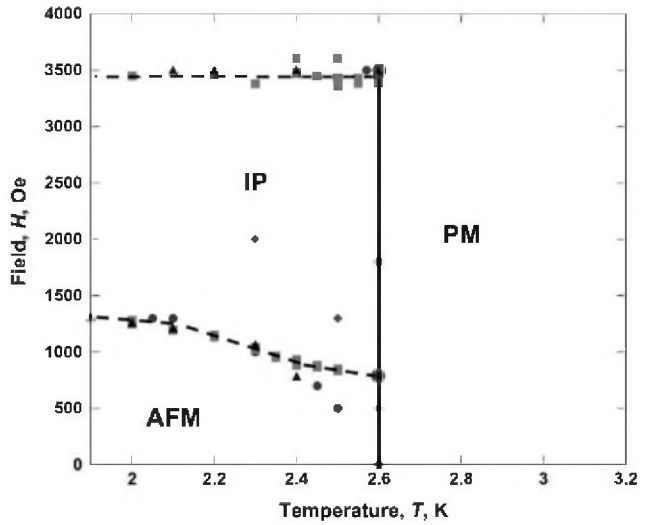

Fig. 11 $H(T)$ of **1MM + E**: (■) $\chi'(H)$, (●) $\chi'(T)$, (▲) $M(H)$, (◆) $M(T)$ and (○) tricritical points; (- - - -) denotes a first order transition along with the metamagnetic phase boundaries; (—) denotes a second order transition.

Since the relaxation processes occurring in the spin system for **1MM** are unknown, and outside the scope of this study, only the peak maxima for 100 and 1000 Hz $\chi'(H)$ and $\chi'(H)$ as well as the $M(T)$ and $M(H)$ data are used to determine the magnetic phase diagram $H(T)$ for **1MM + E** (Fig. 11).

Phase diagram

The $H(T)$ of **1MM + E** contains three different magnetic phases: an antiferromagnetic, **AFM**, an intermediate **IP**, and a paramagnetic phase, **PM**. First-order metamagnetic phase boundaries (MPB) are present between **AFM–IP** and **IP–PM** phases. The **AFM–IP MPB** between ~900 and ~1100 Oe is the result of ~85% of the spins (*vide infra*) in **1MM + E** having flipped from an antiparallel to a parallel spin arrangement with respect to the applied field. The remaining ~15% of the spins do not flip until the **IP–PM MPB** at ~3500 Oe. This corresponds to the bump observed in the 2 K $M(H)$ data (Fig. 6b,d) between 3500 and 4000 Oe, along with the peak observed in the same region for $\chi'(H)$. The genesis of the initial switching of the ~85% of the spins is unknown. Review of the crystal structure[11] fails to reveal features that might account for a higher field needed to flip some of the spins. Given the small fraction of spins flipping at higher fields differences with normal spins can be especially subtle and require correlation with the nuclear and magnetic crystal structures to find them. Unfortunately, the magnetic structure of **1MM** is not yet known.

In contrast, the **AFM–PM** and **IP–PM** phase transitions at 2.6 K are both second order transitions. The two tricritical points, T_t, are estimated to occur at 2.6 K and ~900 and ~3500 Oe. More precise values for the T_ts cannot be determined from the data available from the polycrystalline samples, as suitable single crystals cannot be synthesized for study. Hence, based on previously reported $H(T)$ phase diagrams, they were positioned on the diagram as noted. The lower field T_t is due to the first metamagnetic phase intersecting **IP** and **PM** phases, while the higher field T_t is due to the second metamagnetic boundary intersecting with **IP** and **PM**.

Heat capacity, $C_p(T)$, measurements were done on **1MM** as a function of H below 5000 Oe (Fig. 5).[25] At $H = 0$, a peak in $C_p(T)$ at 2.4 K was observed, which is in good agreement with a previous study[26] and the 2.55 K ordering temperature for **1MM**.[8] Surprisingly, as the ordering temperature for **1MM** was field dependent, as evidenced by the change in the field-dependent maximum in $\chi'(T)$, it was anticipated that the temperature at which the peak in the $C_p(T)$ data occurs for **1MM** would also be as field dependent.[27] This is reported for the antiferromagnet γ-nitrophenyl nitronyl nitroxide (T_N = 0.65 K),[28] in which the maximum in $C_p(T)$ data changes with increasing applied field. Hence, it was unexpected that the 2.4 K peak in $C_p(T)$ data for **1MM** was independent of H.[29] Nonetheless, a field-independent peak was also reported for the ferrimagnet $(NBu_4)[Fe^{II}Fe^{III}(ox)_3]$.[30]

Conclusion

[FeCp*$_2$][TCNQ] forms three different polymorphs with different magnetic ground states: a paramagnet; a ferromagnetic, **1FO**, with T_c = 3.1 K; and a metamagnet, **1MM** with T_c = 2.5 ± 1 K. Alignment of **1FO** and **1MM** crystallites parallel to the applied magnetic field did not effect T_c, but allowed for the detailed magnetic properties of both to be determined.

The 2 K $M(H)$ of **1FO** was characteristic of a ferromagnet with H_{cr} ~ 50 Oe and a remanent magnetization of 1900 emu Oe mol^{-1} at 2 K. **1FO** exhibits frequency independent $\chi'(H)$ and $\chi''(H)$ components in zero applied field consistent with a ferromagnetic state. T_c = 3.1 K for **1FO** and agreed with the previous T_c (175 Hz) of 3.0 K.[11] $C_p(T)$ data for **1FO** had a peak maximum at 3.0 K, in excellent agreement with the peak in $\chi'(T)$ data.

1MM + E was determined from the hysteresis at 2 K to be significantly, but not completely, aligned parallel with the applied field. However, **1MM + E** exhibited different $M(H)$, $\chi'(T)$, and $\chi''(T)$ data than **1MM** indicating that alignment of the crystals enabled the detailed magnetic properties of **1MM** to be observed that were not observed for unaligned samples. Ordering temperatures observed as a function T, H, and f enabled determination of the $H(T)$ phase diagram for **1MM + E**. **1MM + E** has three phases: antiferromagnetic (**AFM**), intermediate (**IP**) and paramagnetic (**PM**) phases, containing two metamagnetic phase boundaries. These boundaries result from ~85% of the **1MM + E** spins flipping from an antiparallel to a parallel spin arrangement at the first boundary (~900 Oe), while the remaining 15% flip at the second boundary (~3500 Oe).

Stable model systems with profound differences in their magnetic properties, but structurally well characterized to be quite similar, and solvent free, are rare, and consequently will serve as important model systems for future theoretical studies. [FeCp*$_2$][TCNQ] has two polymorphs, **1MM** and **1FO**, whose minimal structural differences lead to significantly different cooperative magnet behaviors. The detailed magnetic characterization of each phase herein provides the basis for

theorists to understand the subtle cooperative interactions that lead not only magnetic ordering, but also the sign of the ordering.

Acknowledgements

We gratefully acknowledge the insightful discussions with Arthur J. Epstein (The Ohio State University) and Michio Sorai (Osaka), and the continued partial support from the U.S. DOE (No. DE FG 03-93ER45504), the AFOSR (No. F49620-03-1-0175), and Spanish MAT2004-03395-C02-01.

References

1 J. S. Miller, *Adv. Mater.*, 1990, **2**, 98.
2 J. M. Williams, J. R. Ferraro, R. J. Thorn, K. D. Carlson, U. Geiser, H. H. Wang, A. M. Kini and M. H. Wangbo, in *Organic Superconductors. Synthesis, Structure, Properties and Theory*, ed. R. N. Grimes, Prentice Hall, Englewood Cliffs, New Jersey, USA, 1992.
3 S. J. Blundell and F. L. Pratt, *J. Phys.: Condens. Matter*, 2004, **16**, R771; V. I. Ovcharenko and R. Z. Sagdeev, *Russ. Chem. Rev.*, 1999, **68**, 345; M. Kinoshita, *Philos. Trans. R. Soc. London, A*, 1999, **357**, 2855; J. S. Miller and A. J. Epstein, *Chem. Commun.*, 1998, 1319; J. S. Miller and A. J. Epstein, *Chem. Eng. News*, 1995, **73**, 40, 30; J. S. Miller and A. J. Epstein, *Angew. Chem., Int. Ed. Engl.*, 1994, **33**, 385; M. Kinoshita, *Jpn. J. Appl. Phys.*, 1994, **33**, 5718; D. Gatteschi, *Adv. Mater.*, 1994, **6**, 635.
4 J. S. Miller, A. J. Epstein and W. M. Reiff, *Mol. Cryst. Liq. Cryst.*, 1985, **120**, 27.
5 J. S. Miller, *Adv. Mater.*, 2002, **14**, 1105.
6 J. S. Miller, J. C. Calabrese, H. Rommelmann, S. Chittipeddi, A. J. Epstein, J. H. Zhang and W. M. Reiff, *J. Am. Chem. Soc.*, 1987, **109**, 769; J. S. Miller, J. C. Calabrese, A. J. Epstein, R. W. Bigelow, J. H. Zhang and W. M. Reiff, *J. Chem. Soc., Chem. Commun.*, 1986, 1026.
7 S. Chittipeddi, K. R. Cromack, J. S. Miller and A. J. Epstein, *Phys. Rev. Lett.*, 1987, **58**, 2695.
8 G. A. Candela, L. J. Swartzendruber, J. S. Miller and M. J. Rice, *J. Am. Chem. Soc.*, 1979, **101**, 2755.
9 J. S. Miller, J. H. Zhang, W. M. Reiff, L. D. Preston, A. H. Reis, E. Gerbert, M. Extine, J. Troup and M. D. Ward, *J. Phys. Chem.*, 1987, **91**, 4344.
10 G. T. Yee and J. S. Miller, *Magnetism—Molecules to Materials*, ed. J. S. Miller and M. Drillon, Wiley-VCH, Mannheim, 2004, vol. 5, p. 223; V. Gama and M. T. Duarte, *Magnetism—Molecules to Materials*, ed. J. S. Miller and M. Drillon, Wiley-VCH, Weinheim, 2004, vol. 5, p. 1; E. Coronado, J. R. Galán-Mascarós and J. S. Miller, in *Comprehensive Organometallic Chemistry III*, Elsevier, Amsterdam, 2006, in press.
11 W. E. Broderick, D. M. Eichhorn, X. Liu, P. J. Toscano, S. M. Owens and B. M. Hoffman, *J. Am. Chem. Soc.*, 1995, **117**, 3641–3642.
12 J. S. Miller and A. J. Epstein, *J. Am. Chem. Soc.*, 1987, **109**, 3850.
13 E. Stryjewski and N. Giordano, *Adv. Phys.*, 1977, **26**, 487.
14 (*a*) I. S. Jacobs and P. E. Lawrence, *Phys. Rev.*, 1967, **164**, 866 and references therein; (*b*) C. S. Koonce, B. W. Mangum and D. D. Thornton, *Phys. Rev. B*, 1971, **4**, 4054; (*c*) M. K. Saha, M. C. Morón, F. Palacio and I. Bernal, *Inorg. Chem.*, 2005, **44**, 1354.
15 (*a*) Y. Shapira and S. Foner, *Phys. Rev. B*, 1970, **1**, 3083; (*b*) A. Paduan-Filho, F. Palacio and R. L. Carlin, *J. Phys.*, 1978, **39**, L279; (*c*) F. Palacio, A. Paduan-Filho and R. L. Carlin, *Phys. Rev. B*, 1980, **21**, 296; (*d*) A. Paduan-Filho, C. C. Becerra and F. Palacio, *Phys. Rev. B*, 1991, **43**, 11107; (*e*) J. Campo, F. Palacio, M. C. Morón, C. C. Becerra and A. Paduan-Filho, *J. Phys.: Condens. Matter*, 1999, **11**, 4409.
16 (*a*) D. M. Duggan and D. N. Hendrickson, *Inorg. Chem.*, 1975, **14**, 955; (*b*) K. D. Warren, *Struct. Bonding*, 1976, **45**, 45; (*c*) R. Prins, *Mol. Phys.*, 1970, **19**, 602; (*d*) J. H. Ammeter, *J. Magn. Reson.*, 1978, **30**, 299; (*e*) J. S. Miller, D. T. Glatzhofer, D. M. O'Hare, W. M. Reiff, A. Chackraborty and A. J. Epstein, *Inorg. Chem.*, 1989, **27**, 2930.
17 This synthesis for **1FO** proved to be the most successful in obtaining 100% **1FO**; however, other syntheses yielded a mixture of **1FO** and **1MM**.
18 E. J. Brandon, D. K. Rittenberg, A. M. Arif and J. S. Miller, *Inorg. Chem.*, 1998, **37**, 3376.
19 Actual mass of **1MM** used was 16.2 mg and eicosane was 29.2 mg. Total mass placed in gel cap was 41.3 mg, thus the true sample size of **1** is between 12.1 and 16.2 mg. For purposes of working up the magnetic data the sample size is taken to be 15 mg.
20 (*a*) A. L. M. Bogaarts, B. van Laar, A. C. Botterman and W. J. M. de Jonge, *Phys. Lett.*, 1972, **41**, 411; (*b*) it is very anomalous that neither metamagnetic nor spin-flop phase transitions exhibit hysteresis (see ref. 15(*d*) and references therein).
21 (*a*) L. Holmes and M. Schieber, *Phys. Rev.*, 1968, **167**, 449; (*b*) A. Herwijer, W. J. M. de Jorge, A. C. Botterman, A. L. M. Bongaarts and J. A. Cowen, *Phys. Rev. B*, 1972, **5**, 4618; (*c*) J. E. Battison, A. Kasten, M. J. M. Leask and J. B. Lowry, *Solid State Commun.*, 1975, **17**, 1363.
22 D. K. Rittenberg, K-i. Sugiura, Y. Sakata, S. Mikami, A. J. Epstein and J. S. Miller, *Adv. Mater.*, 2000, **12**, 126.
23 M. L. Taliaferro, T. D. Selby and J. S. Miller, *Chem. Mater.*, 2003, **15**, 3602; Z. J. Huang, F. Cheng, Y. T. Ren, Y. Y. Xue, C. W. Chu and J. S. Miller, *J. Appl. Phys.*, 1993, **73**, 6563.
24 J. Mydosh, *Spin Glasses: An Experimental Introduction*, Taylor & Francis, London, 1993, pp. 64–76.
25 The experiment was not done on **1MM + E** because there was no way to account for the eicosane.
26 M. Nakano and M. Sorai, *Mol. Cryst. Liq. Cryst.*, 1993, **233**, 161.
27 The field independent $C_p(T)$ data were verified on two different samples.
28 Y. Nakazawa, M. Tamura, N. Shirakawa, D. Shiomi, M. Takahashi, M. Kinoshita and M. Ishikawa, *Phys. Rev. B*, 1992, **46**, 8906.
29 This experiment was repeated 3 times with 3 different samples of **1MM**, each time producing the same results.
30 A. Bhattacharjee, K. Saito and M. Sorai, *Solid State Commun.*, 2000, **113**, 543.

